The Journal of Microbiology (2012) Vol. 50, No. 3, pp. 409–418
DOI 10.1007/s12275-012-1440-y

Disruption of *SCO5461* Gene Coding for a Mono-ADP-Ribosyltransferase Enzyme Produces a Conditional Pleiotropic Phenotype Affecting Morphological Differentiation and Antibiotic Production in *Streptomyces coelicolor*§

Krisztina Szirák, Judit Keserű, Sándor Biró, Iván Schmelczer, György Barabás, and András Penyige*

Department of Human Genetics, Medical and Health Science Center, University of Debrecen, Debrecen, Nagyerdei krt 98, H-4032, Hungary

(Received September 2, 2011 / Accepted March 5, 2012)

The *SCO5461* gene of *Streptomyces coelicolor* A3(2) codes for an ADP-ribosyltransferase enzyme that is predicted to be a transmembrane protein with an extracellular catalytic domain. PCR-targeted disruption of the gene resulted in a mutant that differentiated normally on complex SFM medium; however, morphological differentiation in minimal medium was significantly delayed and this phenotype was even more pronounced on osmotically enhanced minimal medium. The mutant did not sporulate when it was grown on R5 medium, however the normal morphological differentiation was restored when the strain was cultivated beside the wild-type *S. coelicolor* M145 strain. Comparison of the pattern of ADP-ribosylated proteins showed a difference between the mutant and the wild type, fewer modified proteins were present in the cellular crude extract of the mutant strain. These results support our previous suggestions that protein ADP-ribosylation is involved in the regulation of differentiation and antibiotic production and secretion in *Streptomyces*.

Keywords: *Streptomyces*, mono-ADP-ribosyltransferase, protein ADP-ribosylation, morphological differentiation, actinorhodin production and secretion

Introduction

Streptomyces species are Gram-positive soil bacteria, well known for their complex life cycle. On solid medium the network of vegetative hyphae, the substrate mycelium, gives rise to aerial hyphae that subsequently undergo septation to form spores (Chater and Losick, 1997). The regulation of the morphological differentiation process is coupled to the production of secondary metabolites, such as antibiotics (Chater and Losick, 1997; Chater, 2006). *Streptomyces coelicolor* A3(2), the model streptomycete, produces several antibiotics, among them the blue-pigmented actinorhodin that is secreted by the *act* transport system (Fernández-Moreno *et al.*, 1991).

Several regulatory genes of morphological differentiation and antibiotic production have been characterized in *S. coelicolor* (Chater and Losick, 1997; Chater, 2006; Flärdh and Buttner, 2009). Complete understanding of the regulation of differentiation and antibiotic production, however, would also require the characterization of posttranslational regulatory mechanisms. Previously, we have reported the presence of protein mono-ADP-ribosylation in *S. griseus* and *S. coelicolor* A3(2) (Penyige *et al.*, 1996; Shima *et al.*, 1996; Penyige *et al.*, 2009). Protein mono-ADP-ribosylation – a post-translational protein modification mechanism – is catalyzed by mono-ADP-ribosyltranferase (ADPRTase) enzymes that transfer the ADP-ribose moiety of β-NAD^+ to a specific amino acid side chain of a protein. ADP-ribosylation is a reversible regulatory mechanism; the inhibitory effect of this modification on protein function can be reversed by removal of the ADP-ribose moiety by ADP-ribose-protein glycohydrolases (Lowery and Ludden, 1990; Ludden, 1994).

The best-known mono-ADPRTases are bacterial toxins, such as cholera, diphtheria, and pertussis toxins, which exclusively act on eukaryotic target proteins (Ueda and Hayaishi, 1985). Endogenous ADPRTases have also been detected in various prokaryotes (Ueda and Hayaishi, 1985; Lowery and Ludden, 1990; Eastman and Dworkin, 1994; Geipel *et al.*, 1996; Huh *et al.*, 1996; Penyige *et al.*, 1996; Serres and Ensign, 1996). ADP-ribosylation of DNA on the amino group at *N*2 of 2'-deoxyguanosine by pierisins, apoptosis-inducing cytotoxic proteins of *Pieris rapae* and *P. brassicae* was also described (Watanabe *et al.*, 2004). Pierisins show homology to the mosquitocidal toxin produced by *Bacillus sphaericus* (Reinert *et al.*, 2006).

Although similarities between the primary sequences of ADPRTases are usually very limited, their structural conservation is high. Prokaryotic ADPRTases fall into two broad groups – the diphtheria toxin (DT) group and the cholera toxin (CT) group – based on the characteristics of the conserved consensus sequences (Nagahama *et al.*, 2000; Holbourn *et al.*, 2006). All ADPRTases share three conserved regions that form the NAD^+-binding and catalytic site: (i) region 1, which contains a conserved Arg (in the DT

*For correspondence. E-mail: penyige@med.unideb.hu; Tel.: +36-52-416-531; Fax: +36-52-416-531
§Supplemental material for this article may be found at http://www.springer.com/content/120956

group His replaces Arg) in a β sheet, and which is involved in the formation of the NAD^+ binding site and active-site integrity; (ii) region 2, containing the aromatic-hydrophobic-Ser-Thr-Ser motif (replaced by two Tyr residues in the DT group) that is characterized by a β sheet followed by an α-helix important for positioning the NAD^+ substrate; and (iii) region 3, the ADP-ribosylating turn-turn (ARTT) loop that contains the strictly conserved catalytic glutamate, which is associated with a nonpolar β strand responsible for the transferase activity (Domenighini and Rappuoli, 1996; Bazan and Koch-Nolte, 1997; Han and Tainer, 2002). A search for the consensus motifs common to ADPRTases in the genome sequence of *S. coelicolor* A3(2) M145 helped us to identify two genes coding for putative ADPRTases, the *SCO5461* gene and the *M. smegmatis arr* ortholog *SCO2680* (Baysarowich *et al.*, 2008).

Here, we report the construction and phenotypic characterization of the *S. coelicolor ΔSCO5461::apr* null mutant. Our data indicate that disruption of *SCO5461* gene results in a pleiotropic conditional phenotype. It affects the timing of morphological differentiation, and the production and secretion of actinorhodin, suggesting that protein ADP-ribosylation is involved in the regulation of differentiation as well as antibiotic production and export in *S. coelicolor*.

Materials and Methods

Bacterial strains, plasmids, and growth conditions

The following media were used for the growth of *S. coelicolor* M145, M145 ΔSCO5461::*apr* and the complemented mutant M145 *ΔSCO5461::apr*/pWHE1 strains: mannitol soy flour medium (SFM); supplemented solid minimal medium (SMMS); SMMS containing 10% w/v sucrose (SMMS+); R5 medium (SMM) (Kieser *et al.*, 2000). To analyze antibiotic production, *S. coelicolor* M145 and its *ΔSCO5461::apr* mutant were cultivated for one week on sterile filters (Paraplan nitrocellulose, 0.2 μm) applied to the surface of solid medium (R5, SMMS, and SMMS+). *Escherichia coli* DH5α was used as the host for cosmid cloning. *E. coli* BW21153/pIJ790 was used as a host for λ RED recombination-based PCR-targeted gene disruption (Gust *et al.*, 2003). *E. coli* ET12567/pUZ8002 was used as the donor in conjugational DNA transfer into *S. coelicolor* M145.

E. coli strains were cultivated in Luria-Bertani and SOB liquid and agar medium (Kieser *et al.*, 2000). Apramycin (50 μg/ml), chloramphenicol (25 μg/ml), kanamycin (50 μg/ml), thiostrepton (8 μg/ml) were added to growth media as required. The *E. coli* HB101 strain used for plasmid construction was cultured at 37°C. The pWHM3 (Amp^R, $Thio^R$) vector (Vara *et al.*, 1989) was used for complementation. *In vitro* DNA manipulations were done by standard genetic techniques (Sambrook *et al.*, 1989). The St3D11 cosmid containing the *SCO5461* gene was a generous gift from the John Innes Centre, Norwich, UK.

Disruption of *SCO5461* in *S. coelicolor* M145

PCR targeted mutagenesis as described previously was used to disrupt the chromosomal *SCO5461* gene with an apramycin resistance marker, *apr* (*aac(3)IV*) (Gust *et al.*, 2003). The following primers were used to amplify the required *apr-oriT* cassette from plasmid pIJ773 according to the ReDirect procedure (www.streptomyces.org.uk/redirect): SCO5461 Forw 5′-CGGAATGCGTCGCTCCGCGGCCGGG TCGTATCCGCATGattccggggatccgtcgacc-3′ and SCO5461 Rev 5′-CGCTGTTCCTGCGCCCCTGAGCCAGGACGCC GTGTCATgtaggctggagctgcttc-3′. The PCR product was introduced into *E. coli* BW21153/pIJ790 harboring the cosmid St3D11 and expressing the λ RED recombinase system. The resulting recombinant cosmid, carrying *SCO5461::apr* instead of *SCO5461*, was introduced into *S. coelicolor* M145 by conjugation using *E. coli* ET12567/pUZ8002 (Gust *et al.*, 2003). The apramycin-resistant, kanamycin-sensitive exconjugants were selected, and gene disruption was confirmed by PCR using Str1-5′-GCCACCTACGGTGAGAA-3′ and Str2 5′-GGACGAGGGATGGGTACG-3′ primers coupled to restriction fragment length polymorphism analysis (RFLP) of the PCR product using *Xho*I enzyme.

Complementation of the *SCO5461* mutant

Complementation of the M145 *ΔSCO5461::apr* mutant was achieved using the plasmid pWHM3. The entire open reading frame of the *SCO5461* gene was amplified by PCR using primers 5461*Hin*dIII*Start* 5′-CAGGAAGCTTGC*ATG*atcA CCactagtctg-3′ and 5461*Eco*RI*Stop*-5′-CAATGAATTCG*T CA*GTGCCAGGGCTGGTAG-3′, with *S. coelicolor* M145 genomic DNA as template. The amplification conditions were as follows: an initial denaturation at 95°C for 5 min, followed by 35 cycles of 45 sec at 95°C, 45 sec at 67°C and 1 min 30 sec at 72°C followed by a final 10 min extension at 72°C. The 636 bp PCR product was inserted between the *Hin*dIII and *Eco*RI sites of pWHM3 in frame with the weak *lacZ* promoter (K. Chater personal communication) to obtain pWHE1.

The resulting pWHE1 plasmid was cloned in *E. coli* HB101 cells and the construct was verified by PCR and RFLP analysis. pWHE1 was then transformed into *S. coelicolor* M145 *ΔSCO5461::apr* to obtain the thiostrepton resistant complemented *S. coelicolor* M145 *ΔSCO5461::apr*/pWHE1 strain (Kieser *et al.*, 2000).

Protein ADP-ribosylation assay

The assay was done according to Penyige *et al.* (1996) with slight modifications. In brief, 32 h mycelium grown on cellophane-covered R5 plates was suspended in ADP-ribosylation buffer (20 mM Tris/HCl; pH 7.4, 50 mM NaCl, 2.0 mM $MgCl_2$, 1 mM dithiothreitol, and 2 μg/ml protease inhibitor cocktail and sonicated for 2 min at 0°C. After centrifugation for 20 min at 30,000×*g* at 4°C, the supernatant was supplemented with 25 μM ADP-ribose and 10 μM β-[adenylate-^{32}P]NAD^+ (1.85×10^6 Bq/100 μl sample). Following incubation at 30°C for 30 min 100 μl ice cold 20% (w/v) trichloroacetic acid (TCA) was added and proteins precipitated at 0°C were collected by centrifugation (for 5 min at 12,000×*g*). The pellet was washed twice with 10% (w/v) TCA, then with diethyl ether. Proteins were solubilised overnight at 4°C in 40 μl 2× concentrated electrophoresis sample buffer mixed with 5 μl 5% (w/v) SDS. Before electrophoresis, samples were heated at 90°C for 5 min, ADP-ribosylated proteins

were separated by SDS-PAGE using 5% (w/v) stacking gel and a 13% (w/v) separating gel with a constant voltage of 200 V. Proteins from the gel were electrophoretically blotted to Immobilon P transfer membrane (Millipore, PVDF type, 1.45 µm pore size,) in a semi-dry transfer assembly. The blots were air-dried and the labeled proteins were detected by a phosphor image analyzer (MolecularDynamics Phosphor-Imager SI).

Identification of the modifying group

Proteins in 500 µl cellular crude extract of *S. coelicolor* M145 were ADP-ribosylated and TCA precipitated as described above. The pellet was washed three times with diethylether and resuspended in 500 µl 10 mM KOH containing 6 M guanidine-HCl. A 100 µl aliquot was immediately removed from the sample in order to determine its radioactivity by liquid scintillation (PerkinElmer Liquid Scintillation Analyzer 2800 TR). For alkaline hydrolysis of ^{32}P-labeled proteins the sample was incubated for 3 h at 27°C, then proteins were precipitated with $HClO_4$ at 0°C overnight (Jouanneau *et al.*, 1989; Ochi *et al.*, 1992). The sample was centrifuged for 30 min at 12,000×*g* at 4°C. Radioactivity in the supernatant and in the pellet was determined by liquid scintillation assay. 90 ml of the supernatant was spiked with 10 ml nucleotide standard solution containing ADP, AMP, ADP-ribose (100 nM each) and was analyzed by high perform-

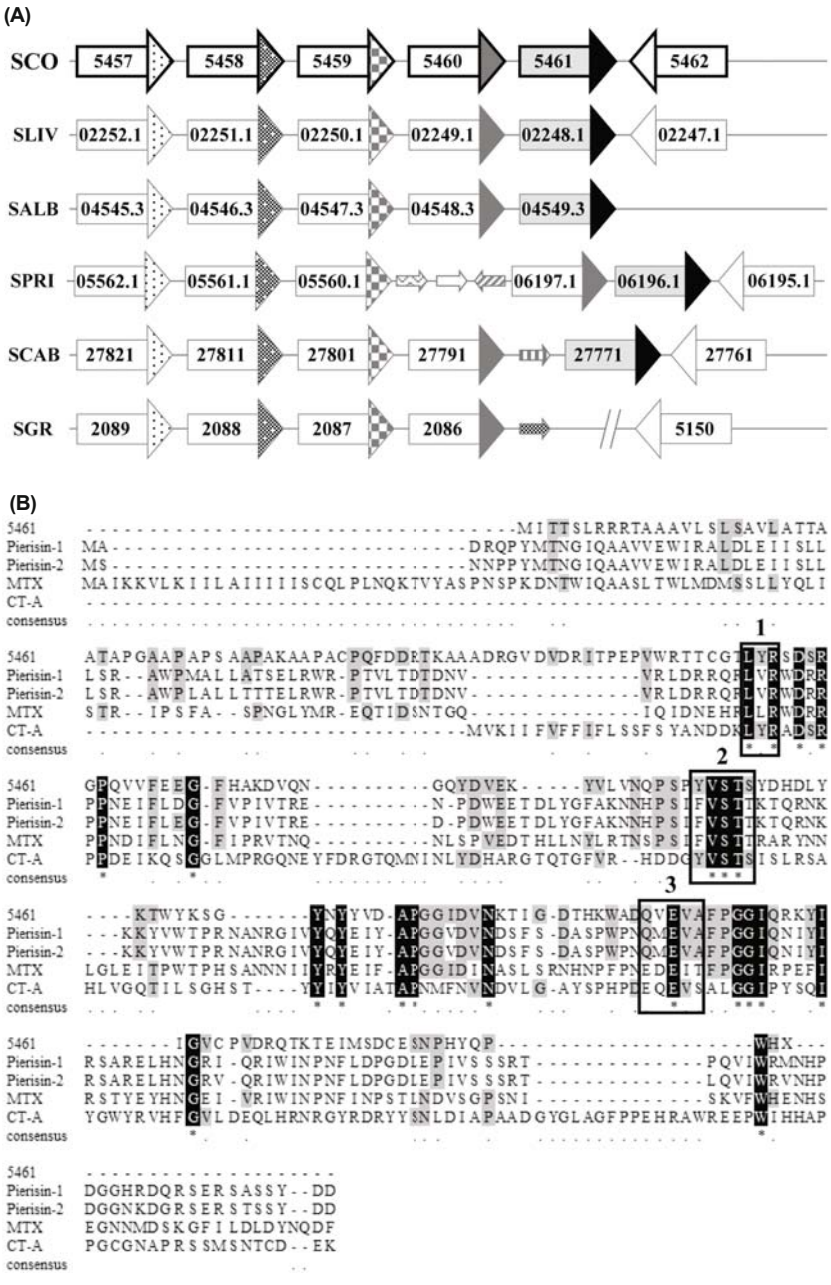

Fig. 1. **(A) Organization of the genomic region containing the *SCO5461* gene in *S. coelicolor* (SCO) and the alignment of the conserved orthologues in *S. lividans* (SLIV), *S. albus* (SALB), *S. pristinaespiralis* (SPRI; the numbers are taken from the original contigs), *S. scabies* (SCAB), and *S. griseus* (SGR).** Identical shaded patterns refer to the respective orthologues. (B) Multiple-amino acid sequence alignment of mono-ADP-ribosyltransferases: SCO5461 from *S. coelicolor*; Pierisin-1 and Pierisin-2 from *Pieris rapae* and *P. brassicae*, respectively; mosquitocidal toxin from *B. sphaericus* (MTX) and cholera toxin A subunit from *Vibrio cholerae* (CT-A). The framed, numbered sequences represent the three essential ADPRTase motifs. Outlined amino acids are homologous with the sequence of SCO5461. The conserved amino acids are highlighted in black. The amino acids that cannot be found in all ortologues are highlighted in light gray.

ance liquid chromatography (Waters 650E Solvent Delivery System) with UV detection at 254 nm. Nucleotides were separated by reversed-phase chromatography, on a BST Si-100-S 10 C18 (250 mm × 4.6 mm i.d., 5.0 µm particle size) column at a flow rate of 1.8 ml/min, with a gradient of buffer A to buffer B. Buffer A consisted of 10% methanol in 10 mM KH_2PO_4 (pH 6.0). Buffer B consisted of 50 mM KH_2PO_4, (pH 6.0). 0.5 ml fractions were collected during the elution and the radioactivity in the fractions were determined by liquid scintillation. This experiment was done in triplicate.

Sequence identification and alignments; secondary structure prediction and 3D structure prediction

The putative amino acid sequence of SCO5461 was obtained from the genome database of *S. coelicolor* (http://streptomyces.org.uk/). Sequence analysis and alignments were performed using a PSI-BLAST search through the NCBI web server (www.ncbi.nlm.nih.gov/BLAST). Secondary structure predictions were made using SSPRED software (www.coot.embl.de/~fmilpetz/SSPRED) and TMpred server (http://www.ch.embnet.org). Signal peptide analysis was done using the SignalP program (www.cbs.dtu.dk/services/SignalP); TatFind and TatP software (www.signalfind.org and www.cbs.dtu.dk/services/TatP, respectively). Protein 3D structure was predicted by using the $(PS)^2$ modeling software (http://ps2.life.nctu.edu.tw).

Databases

The following databases were used for genomic sequence analysis of the various *Streptomyces* strains: http://www.broadinstitute.org (for *S. lividans*; *S. albus*; *S. pristinaespiralis*); http://streptomyces.org.uk (for *S. coelicolor*; *S. scabies*; *S. griseus*; *S. avermitilis*; *S. clavuligerus*; *S. venezuelae*).

Results

Characterization of SCO5461

The *SCO5461* gene is located in the central core region of the chromosome of *S. coelicolor*, with four upstream genes (*SCO5457-SCO5460*) lying in the same orientation. Although this arrangement and the fact that there are similarly oriented orthologues of these genes in genomes of several *Streptomyces* strains (Fig. 1A) might suggest that the five genes form an operon, we cannot confirm this suggestion. In genomes of more distant relatives of *S. coelicolor* such as *S. pristinaespiralis* or *S. scabies*, the arrangement of the first three genes is strictly conserved. However, one or more genes can be found inserted between the third and fourth gene or the fourth gene and the *SCO5461* orthologue (Fig. 1A). There are *Streptomyces* strains that do not contain an orthologue gene for *SCO5461*, such as *S. griseus*, *S. clavuligerus*, *S. avermitilis*, and *S. venezuelae* (data not shown).

SCO5461 is annotated as a putative secreted protein of 204 amino acids with a calculated molecular mass of 22,386 Da. PSI-BLAST searches showed that among the functionally characterized proteins, the SCO5461 protein is most similar to ADP-ribosylating toxins of other prokaryotes and eukaryotes (Fig. 1B). SCO5461 shows homology to the N-terminal catalytic domain of the DNA modifying ADP-ribosyltransferases pierisin-1 and pierisin-2 from *Pieris rapae* (34% identity, 43% positives), and *P. brassicae* (35% identity, 44% positives), respectively. SCO5461 also shows homology to the catalytic domain of the ADP-ribosylating mosquitocidal toxin (MTX; 31% identity, 46% positives) of *Bacillus sphaericus* and also, importantly, to the A subunit of cholera toxin (CtxA; 24% identity, 34% positives) (Fig. 1B).

Multiple sequence alignments revealed that the SCO5461 protein contains the conserved motifs essential for ADPRTase activity (Holbourn *et al.*, 2006). In SCO5461, Leu is found

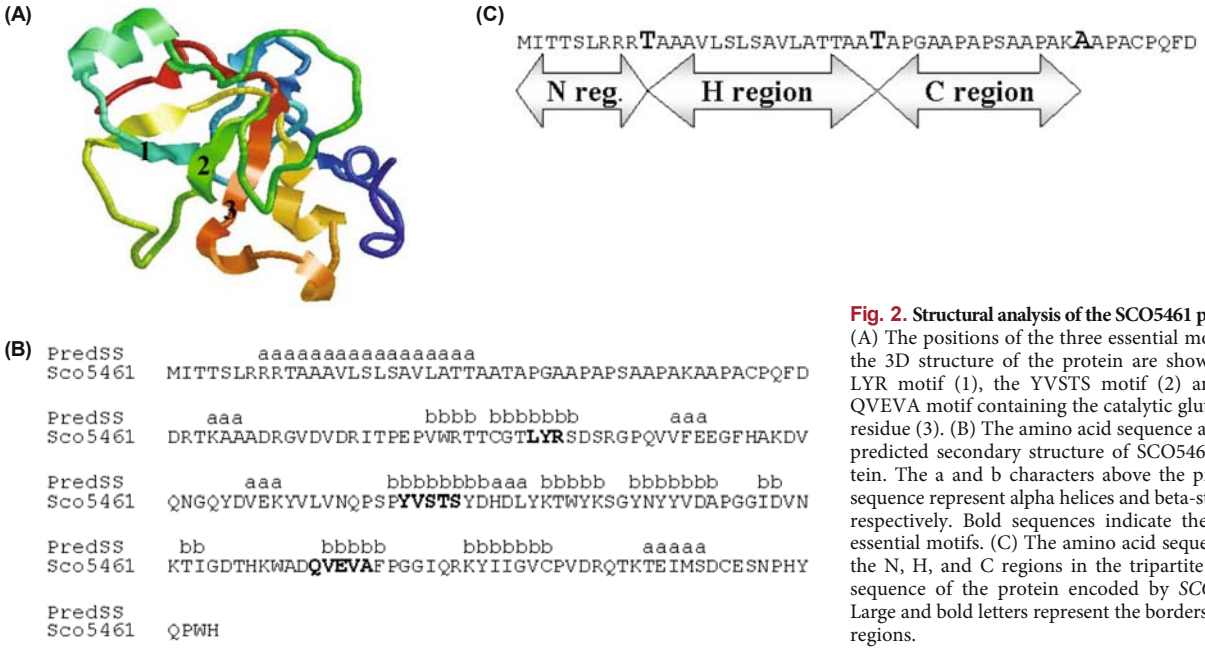

Fig. 2. Structural analysis of the SCO5461 protein. (A) The positions of the three essential motifs in the 3D structure of the protein are shown: the LYR motif (1), the YVSTS motif (2) and the QVEVA motif containing the catalytic glutamate residue (3). (B) The amino acid sequence and the predicted secondary structure of SCO5461 protein. The a and b characters above the primary sequence represent alpha helices and beta-strands, respectively. Bold sequences indicate the three essential motifs. (C) The amino acid sequence of the N, H, and C regions in the tripartite signal sequence of the protein encoded by *SCO5461*. Large and bold letters represent the borders of the regions.

before the conserved *aromatic-R/H* motif that consists of Tyr-80 and Arg-81 (YR). The YVSTS sequence in SCO5461 corresponds to the *aromatic-hydrophobic-S-T-S* motif and the QVEVA sequence corresponds to the ARTT loop. In all members of the CT family, a Glu/Gln residue is found two residues upstream of the catalytic Gln (Holbourn *et al.*, 2006). According to these sequence characteristics, SCO5461 might belong to the CT family of mono-ADPRTases. Interestingly, all orthologues of SCO5461 contain the conserved ADPRTase motifs (Supplementary data Fig. S1).

Due to the great interest in the family of ADP-ribosylating toxins, the 3D structures of several ADPRTases have been reported, including the mosquitocidal toxin from *Bacillus sphaericus* and cholera toxin (Zhang *et al.*, 1995; Reinert *et al.*, 2006). Based on these known structures and the recognized sequence homologies we have predicted the 3D structure of SCO5461 using the PS2 software intended for comparative modeling of protein three-dimensional structures (Fig. 2A). Despite the lack of extended amino acid sequence similarity, the chain fold of the SCO5461 protein corresponds to the core fold of ADPRTases (Fig. 2A). In SCO5461, the conserved LYR and YVSTS motifs are part of two perpendicular β-sheets, while the catalytic Glu-164 is in a loop connecting a β-sheet and an α-helix as in the ARTT loop of CT (Holbourn *et al.*, 2006). As shown in Fig. 2B, the secondary structure of SCO5461 predicted by the SSPRED program fits the predicted 3D structure, since the LYR and YVSTS motifs are part of β-sheets and QVEVA is on the border of an unstructured loop and β-sheet.

In StrepDB, SCO5461 is annotated as a putative secreted protein with possible non-cleavable N-terminal signal. The SignalP (version 3.0) program (http://cbs.dtu.dk/services/SignalP) indeed recognized a tripartite N-terminal signal sequence (1–43 amino acids) in SCO5461, which contains an rrrtaa motif in its N-terminal part that might resemble a twin-arginine translocation (Tat) signal (Fig. 2C) (Li *et al.*, 2005; Widdick *et al.*, 2006). We have used the prediction programs TatFind version 1.4 and TatP version 1.0 to check whether the SCO5461 protein could be a candidate Tat substrate. None of the programs recognized the N-terminal sequence of SCO5461 as a genuine Tat-targeting signal. This conclusion is in accordance with previously reported results that the SCO5461 signal peptide did not mediate the transfer of a reporter protein in *S. coelicolor* M145 (Widdick *et al.*, 2006). Tat signal peptides superficially resemble Sec signal peptides; however, the positively charged K41 residue at the end of the C-region of the suggested signal peptide of the SCO5461 protein (Fig. 2C) might function as a Sec avoidance signal (Li *et al.*, 2005), which could explain the finding that SCO5461 is not secreted in the *S. coelicolor* M145 *ΔtatC* mutant defective in Tat transport (Widdick *et al.*, 2006). The SCO5461 protein, however, is present in the cell-wall fraction in *S. coelicolor* M145, suggesting that SCO5461 might be a transmembrane protein with an extracellular domain (Widdick *et al.*, 2006). This notion is confirmed by several protein secondary structure predictions. As seen in Fig. 2B, the SSPRED software predicted an N-terminal α-helix, which was confirmed among others, by the TMpred server (http://ch.embnet.org). According to TMpred prediction, the SCO5461 protein is a transmembrane protein with a short (9 aa) intracellular domain, an inside to outside transmembrane helix (26 aa) and a longer extracellular domain (27–204 aa) (data not shown).

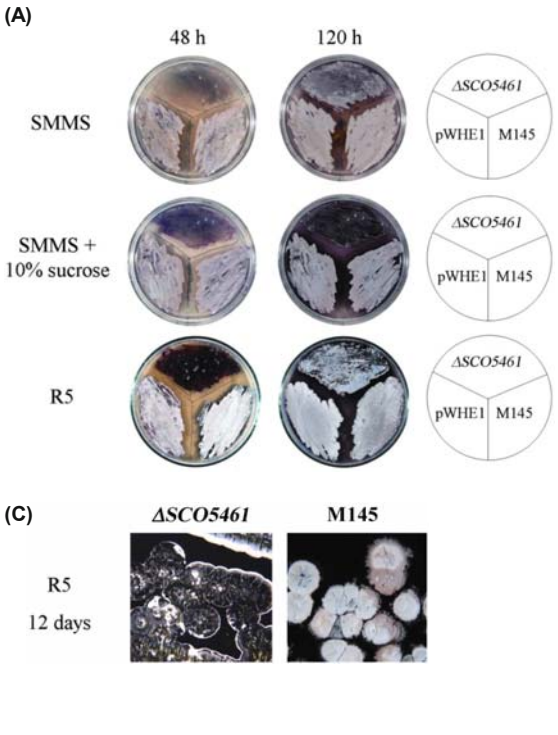

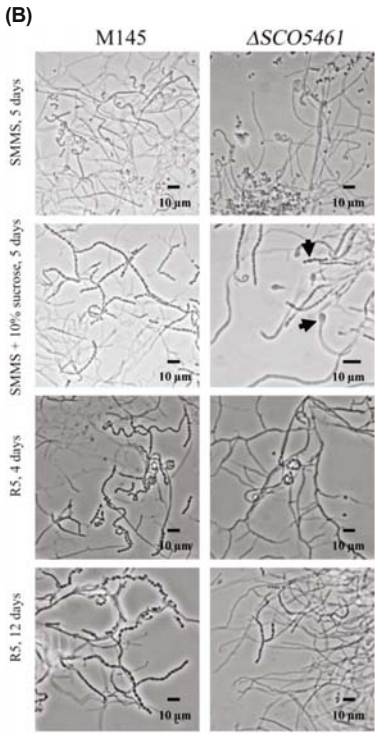

Fig. 3. Disruption of the *SCO5461* gene in *S. coelicolor* affects morphological differentiation. (A) Phenotypes of *S. coelicolor* M145, *S. coelicolor* M145 *ΔSCO5461::arp* mutant (*ΔSCO5461*) and the complemented *S. coelicolor* M145*ΔSCO5461::apr*/pWHE1 (pWHE1) strains grown on SMMS, SMMS+10% sucrose and R5-agar after 48 h and 120 h of cultivation (see details in the text). The drawn schemes depict the arrangement of the three strains on agar plates. (B) Phenotype of the *ΔSCO5461::arp* mutant and the wild-type strain (M145) grown on separate R5-agar plates. The white-grayish surface of solid cultures represents spore production. (C) Representative phase-contrast micrographs of mutant and wild-type cultures grown in SMMS, SMMS+10% sucrose and R5-agar. Abundant aerial hyphae and spore production are obvious in the case of the wild-type M145 strain under all growth conditions. The mutant shows sparse sporulation on SMMS, while abnormal spore chains and swollen hyphal tips (black arrows) are present in the mutant culture grown in SMMS+10% sucrose. On R5 medium, the mutant does not sporulate even after 288 h of cultivation.

Disruption of the *SCO5461* and complementation of the mutant

PCR targeted mutagenesis was used to disrupt the *SCO5461* gene with an apramycin resistance cassette (Gust *et al.*, 2003). Gene replacement was verified by PCR coupled to RFLP analysis of both the recombinant cosmid and the genomic DNA of the apramycin resistant *ΔSCO5461::apr* mutant. For complementation analysis, the PCR product containing the complete *SCO5461* gene was cloned into the *Eco*RI/*Hin*dIII site of pWHM3 creating pWHE1. The construct was transformed into the *S. coelicolor* M145 *ΔSCO5461::apr* mutant, generating the complemented *S. coelicolor* M145*ΔSCO5461::pr*/pWHE1 strain.

Phenotypic analysis of the *ΔSCO5461::apr* mutant: morphological differentiation

Disruption of the *SCO5461* gene resulted in a conditional pleiotropic phenotype. On SFM-agar medium, the phenotype of the null mutant was similar to that of the wild-type strain (data not shown). Since phenotypes of mutants might depend on the growth medium, spores of M145, the M145*ΔSCO5461::apr*/pWHE1 complemented mutant, and the *ΔSCO5461::apr* mutant were streaked onto the following media: SMMS, SMMS supplemented with 10% sucrose (SMMS+) and R5.

On SMMS medium, the M145 *ΔSCO5461::apr* mutant showed delayed morphological differentiation compared to that of *S. coelicolor* M145 and *S. coelicolor* M145*ΔSCO5461::apr*/pWHE1. In 48 h, old cultures of *S. coelicolor* M145 and M145*ΔSCO5461::apr*/pWHE1 produced aerial mycelia and spores, while the mutant had a bald-like appearance. At 120 h, aerial mycelium and spore production were evident in the mutant culture as well; however, spore formation was not as dense as it was in the control culture (Fig. 3A). The applied osmotic stress in SMMS+ even more strongly delayed aerial hyphae production and sporulation. At 120 h, the null mutant displayed sparse aerial mycelium and spore formation (Fig. 3A). After one week of cultivation the mutant sporulated abundantly (data not shown).

The phenotype of the *ΔSCO5461::apr* mutant strain was different when grown on R5 medium. Both the aerial mycelium formation and sporulation were completely suppressed in the mutant growing alone on R5-agar, suggesting that normal ADP-ribosyltransferase activity is required for differentiation on this osmotically enhanced, rich medium. The surface of the colonies of the *ΔSCO5461::apr* mutant had a bald-like appearance but unlike the *bldA* mutant, it produced actinorhodin as a blue color in the medium (shown in Fig. 3B). The morphological differentiation of the *ΔSCO5461::apr* mutant was restored when it was grown beside the wild-type M145 or the *S. coelicolor* M145*ΔSCO5461::apr*/pWHE1 strain on R5-agar (Fig. 3A). The wild-type phenotype was also restored when the mutant was cultivated on a spent R5 medium of the *S. coelicolor* M145 strain (data not shown). It is important to note, that on SMMS and SMMS+ media the mutant sporulated after a longer cultivation period when it was grown in the absence of the wild-type strain (data not shown).

Since the complemented *S. coelicolor* M145*ΔSCO5461::apr*/pWHE1 strain had normal phenotype in all three media, we concluded that in the M145 *ΔSCO5461::apr* strain, the mutant phenotype is due to the disruption of the *SCO5461* gene.

Observations of the M145 *ΔSCO5461::apr* strain under a phase-contrast light microscope confirmed the above-described characteristics. Phenotypes of samples were visualized by growing the cells on cover slips inserted into the agar plates (Kieser *et al.*, 2000). After 5 days of incubation in SMMS medium, aerial mycelium and spore chains were present in the sample of the mutant strain, but spores were less abundant than in the wild-type sample (Fig. 3C). The difference between the wild-type and mutant phenotypes was even more pronounced in SMMS+ medium. In addition to aberrant, unevenly swollen spores, swollen hyphal tips were also frequent in the culture (Fig. 3C). The phenotype of the *ΔSCO5461::apr* strain grown in R5-agar plates, after four days of cultivation, showed mostly undifferentiated mycelium and very few, short spore chains. Only occasional spore chains were formed even after 12 days of cultivation (Fig. 3C).

Antibiotic production

In addition to morphological differentiation defects, the production and secretion of actinorhodin was different in the null mutant. The strains were grown on sterile filters deposited on the surface of the three different solid media. The filters did not allow the growth of the mycelium into the medium. The advantage of this arrangement is that re-

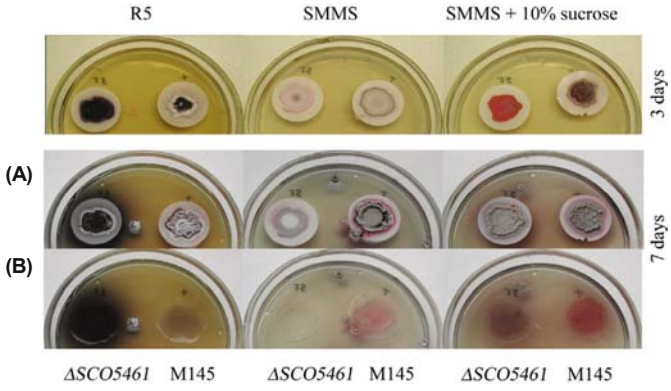

Fig. 4. Effect of *SCO5461* disruption on actinorhodin production and secretion of *S. coelicolor* grown in R5-agar, SMMS, and SMMS+10% sucrose. *S. coelicolor* M145 and the *ΔSCO5461::arp* mutant strains were inoculated on sterile filters positioned on the agar plates. Photographs were taken after 3 and 7 days of cultivation. Actinorhodin secretion was visualized by the removal of the filters from the agar plates. On R5-agar the mutant does not form spores but, as the coloration of the cultures shows, actinorhodin is produced by both strains. However, much more actinorhodin is secreted by the mutant than the wild type after 7 days of cultivation. On SMMS, actinorhodin production started earlier in the mutant according to its pink color, but the mutant did not secrete the antibiotic. On SMMS +10% sucrose both strains produce antibiotics at the same stages. Their different coloration might be due to different intracellular pH values. Both strains secreted the antibiotic into the extracellular space on this medium. (A) and (B) show the same plate, before and after the removal of the filters, respectively.

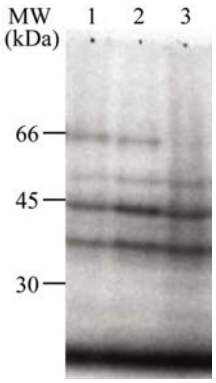

Fig. 5. Comparison of the pattern of ADP-ribosylated proteins of the wild-type M145 strain (lane 1) and the complemented *S. coelicolor* M145*ΔSCO5461::apr*/pWHE1 (lane 2) to that of the *ΔSCO5461::apr* mutant (lane 3). Proteins present in cellular crude extracts of 32 h R5-agar grown cultures were ADP-ribosylated using [^{32}P]NAD$^+$ as substrate. The proteins were resolved by SDS-PAGE, blotted to PVDF filters and analyzed by phosphor-image analyzer. The positions of molecular mass markers (MW) are shown on the left side of the gel.

moval of the filter with the mycelium on it makes it possible to visualize the blue actinorhodin antibiotic secreted into the extracellular environment. On SMMS the mutant mycelium contained a lower amount of actinorhodin than the wild-type strain and it was not secreted into the medium, as the removal of the filter with the mycelium revealed. After three days of cultivation on SMMS+ the mycelium of the two strains differed in their coloration; the mutant strain produced red pigment, while the wild type produced blue. Removal of the filters after seven days of cultivation revealed that the mutant secreted the same amount of actinorhodin into the extracellular environment as the wild type. On R5 the actinorhodin production and secretion by the*ΔSCO5461::apr* strain was greater than that of the wild-type M145 strain (Fig. 4).

Protein ADP-ribosylation

The sequence and 3D structural data suggested that the *SCO5461* gene product is a mono-ADPRTase. To confirm this suggestion, the ADP-ribosylated protein pattern of the wild-type *S. coelicolor* M145 strain was compared to that of the M145 *ΔSCO5461::apr* mutant and the complemented *S. coelicolor* M145*ΔSCO5461::apr*/pWHE1 strain. The three strains were grown on cellophane-covered R5 plates and cell free crude extracts were prepared just before the onset of aerial mycelium formation (32 h) from the mycelial samples resuspended in ADP-ribosylation buffer. Proteins were ADP-ribosylated using [adenylate-^{32}P]-NAD$^+$ and the modified proteins were separated by SDS-PAGE and electroblotted to PVDF filters. Disruption of *SCO5461* resulted in a reduced number of ADP-ribosylated proteins, compared to that of the wild-type strain (Fig. 5), suggesting that *SCO5461* codes for an ADPRTase. Moreover, the pattern of ADP-ribosylated proteins of the complemented strain was identical to that of the wild type. The ADP-ribosylated protein pattern of the mutant, however, did not show dramatic differences, indicating that SCO5461 is not the only ADPRTase in *S. coelicolor*.

To show that the labeled proteins were ADP-ribosylated, the chemical nature of the radioactive group incorporated into proteins from (^{32}P)-labeled NAD$^+$ was determined after alkaline hydrolysis by high performance liquid chromatography (HPLC). Proteins present in the cellular crude extract of the *S. coelicolor* M145 strain following the ADP-ribosylation assay were TCA precipitated and the pellet containing 4.9×10^5 Bq incorporated ^{32}P label was alkaline hydrolized (Jouanneau *et al.*, 1989). The radioactive nucleotide content of the hydrolysate was analyzed with HPLC using a reversed-phase C18 column. The radioactivity of fractions collected during the elution was measured by liquid scintillation. Most of the radioactivity was eluted together with ADP-ri-

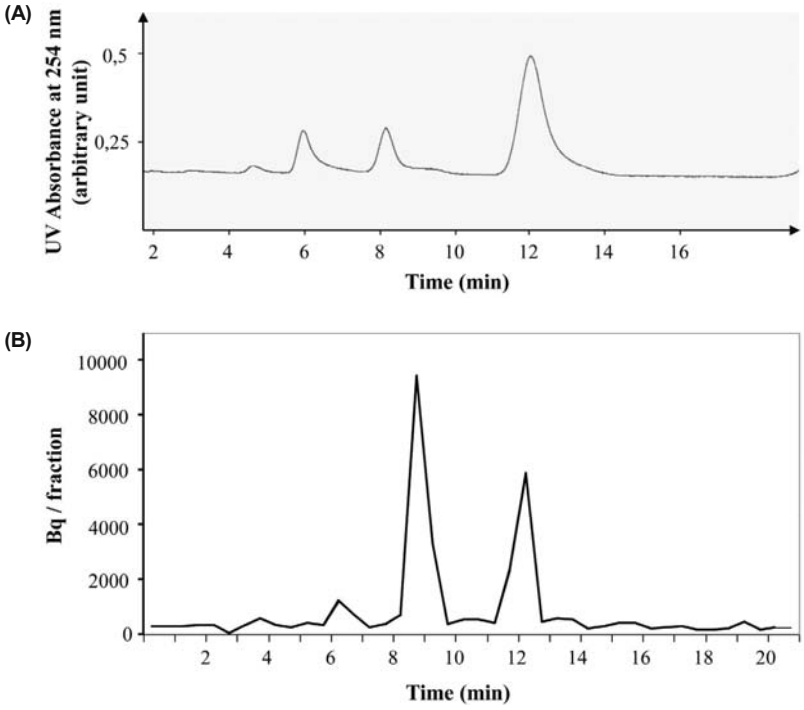

Fig. 6. Reversed-phase HPLC analysis of the alkaline hydrolyzate of *S. coelicolor* M145 proteins previously incubated with [^{32}P]NAD$^+$. The elution pattern of the nucleotides is shown on (A), the sequence of peaks corresponds to ADP, ADP-ribose, and AMP, in that order. The radioactivity in the fractions, collected during the elution of nucleotides was measured by liquid scintillation (B).

bose (58.1%) and AMP (37.4%) (Fig. 6) as expected after alkaline hydrolysis of ADP-ribosylated proteins (Jouanneau *et al.*, 1989; Ochi *et al.*, 1992). A small fraction of the incorporated label was found in ADP (8.1%). The experiment was done in triplicate, a representative result is shown in Fig. 6.

To summarize our results, analysis of the *S. coelicolor ΔSCO5461::apr* mutant shows that SCO5461 probably codes for an ADPRTase enzyme that is involved in the regulation of differentiation, especially under osmotic stress. The absence of the SCO5461 protein affects actinorhodin production in solid cultures.

Discussion

To analyze its physiological role in *S. coelicolor*, the *SCO5461* gene was disrupted with an apramycin cassette using PCR-targeted mutagenesis. *SCO5461* was chosen because our preliminary sequence analysis identified the presence of key motives characteristic for ADPRTase enzymes in the protein coded by the gene. Comparison of the amino acid sequence of the SCO5461 protein to that of known ADPRTase enzymes – pierisins, cholera toxin, and mosquitocidal larval toxin – in a multiple-amino acid sequence alignment analysis supported our suggestion, that *SCO5461* very likely codes for an ADPRTase enzyme. The primary structure of SCO5461 contains (i) the (79)LYR(81) sequence corresponding to the aromatic-R/H motif; (ii) a (119)YVSTS(123) sequence corresponding to the aromatic-hydrophobic-S-T-S motif and (iii) a the (162)QVEVA(166) sequence corresponding to the conserved Q/E-X-E motif essential for ADPRTase activity (Houlbourn *et al.*, 2006). According to these sequence characteristics, SCO5461 belongs to the CT family of mono-ADPRTases (Houlbourn *et al.*, 2006). The absence of a 65 kDa ADP-ribosylated protein in the cytoplasmic fraction of *ΔSCO5461::apr* null mutant that was present in the wild type also supports our hypothesis. We would like to note, that in one of our previous publications we identified an ADP-ribosylated protein with the same molecular mass, and found that protein was the solute-binding subunit of an oligopeptide ABC transporter, coded by the *SCO5477* gene (Penyige *et al.*, 2009).

To strengthen support for our hypothesis, using alkaline hydrolysis and HPLC analysis we were able to show that the radioactivity from [^{32}P]NAD^{+} was incorporated into ADP-ribose, so the radioactively labeled proteins in the sample were really ADP-ribosylated proteins (Ochi *et al.*, 1992). In summary, the homologous sequences and the ADP-ribosylated protein pattern imply the same conclusion, namely that *SCO5461* codes for an ADPRTase enzyme.

Being an endogenous ADPRTase, it is important to determine the exact location of the SCO5461 protein. The N-terminus of SCO5461 contains a putative tripartite signal sequence (length: 42 aa) showing similarity to Tat signal peptides and also superficial resemblance to Sec signal peptides (Stephenson, 2005). It is very likely, however, that SCO5461 is not an extracellular protein, since neither the program TatP nor TATFIND recognized the N-terminal as a Tat-targeting signal and the positively charged K41 residue in the signal peptide might serve as a Sec avoidance signal. Interestingly, in a previous publication the SCO5461 protein was found in the cell wall-cell membrane fraction of the wild-type *S. coelicolor* M145 strain; however, it was absent from the same fraction of a *tat* mutant of the same strain (Widdick *et al.*, 2006). It was also shown that the N-terminal signal peptide of SCO5461 did not mediate the transfer of a reporter agarase gene in the case of the wild-type M145 strain. These data rule out the possibility that SCO5461 is exported to the extracellular space either via the Tat or the Sec pathways. Although the original publication considered SCO5461 as a contamination in the cell wall-cell membrane fraction, we cannot rule out the possibility that SO5461 is a transmembrane protein. *In silico* prediction of the secondary structure of SCO5461 data suggested a transmembrane localization for the SCO5461 protein with a short (9 aa) intracellular stretch, a 26 aa long transmembrane domain, and a 172 aa extracellular domain containing the catalytically important motives. Ecto-ADP-ribosyltransferase enzymes are known to be present on the surface of eukaryotic cells (Ritter *et al.*, 2003).

Recently we have published a list of proteins that were ADP-ribosylated in *S. coelicolor* M145, among them periplasmic solute-binding subunits of several ABC-transporters (Penyige *et al.*, 2009). Previously, Sugawara *et al.* (2002) suggested that ADP-ribosylation of periplasmic proteins might interfere with the transfer of these proteins to the periplasmic compartment. However, in the light of our recent data, we can hypothesize that periplasmic proteins could be ADP-ribosylated by the extracellular domain of SCO5461. Since the previously suggested site for ADP-ribosylation is the same Cys residue that is the site for lipid modification, extracellular ADP-ribosylation of this residue still could interfere with the proper functioning of the modified periplasmic protein (Sugawara *et al.*, 2002).

Disruption of the *SCO5461* gene resulted in a conditional pleiotropic phenotype that was complemented by cloning the *SCO5461* into the *Eco*RI/*Hin*dIII site of the pWHM3 expression vector and introducing the resultant pWHE1 construct into the Δ*SCO5461::apr* null mutant. Phenotypic analysis uncovered a conditional defect in morphological differentiation and antibiotic production. While growing on SFM medium, the *ΔSCO5461::apr* mutant showed no detectable defects, but formation of aerial hyphae and sporulation were delayed on SMMS medium. Although the *S. coelicolor ΔSCO5461::apr* mutant finally produced aerial mycelium and spores, sporulation was not as abundant as that of the wild-type strain. The delay in morphological differentiation was further enhanced when SMMS was supplemented with 10% sucrose. The most dramatic changes in the phenotype of *S. coelicolor ΔSCO5461::apr* mutant were observed on R5-agar, a rich and osmotically enhanced medium. Aerial mycelium formation and sporulation were suppressed in the mutant growing on R5-agar, and the surface of the colonies had a bald-like appearance but, unlike the *bldA* mutant, the *ΔSCO5461::apr* mutant produced actinorhodin. These results suggest, that the normal protein ADP-ribosylation pattern is required for adaptation to osmotic stress conditions.

It is noteworthy, that the normal morphological differen-

tiation was restored when the *ΔSCO5461::apr* mutant was grown beside the wild-type M145 and the complemented *S. coelicolor* M145 *ΔSCO5461::apr*/pWHE1 strain in R5-agar. This extracellular complementation suggests that production or secretion of small diffusible factors required for aerial mycelium formation might be affected by the disruption of the *SCO5461* gene on this medium.

In addition to the defect in morphological differentiation, the production and secretion of actinorhodin is also affected in the constructed null mutant. The mutant produced and secreted more actinorhodin than the wild-type strain when it was grown on R5, and less actinorhodin was produced when it was grown on SMMS and SMMS+ media. Considering the possible extracellular location of the catalytic domain of the SCO5461 protein, the differences in antibiotic secretion might confirm our previous suggestion that ADP-ribosylation of certain subunits of ABC transporter complexes might affect solute transport in *Streptomyces*.

According to our knowledge, this is the first report about a mutational analysis of an endogenous mono-ADP-ribosyltransferase enzyme in Gram-positive bacteria. The results are notable because the phenotype of the *S. coelicolor* M145 *ΔSCO5461::apr* mutant, having pleiotropic defects in morphological differentiation and antibiotic secretion, is in line with our previous suggestions about the involvement of protein ADP-ribosylation in the regulation of differentiation in *Streptomyces* species (Penyige *et al.*, 1996; Shima *et al.*, 1996).

Acknowledgements

We thank Dr. Teréz Márián (Department of Nuclear Medicine, University of Debrecen) for her help in the autoradiography and Dr. Ida Miklós (Department of Genetics and Applied Microbiology, University of Debrecen) for her skillful technical advice on photography with the phase contrast microscope. The authors are also grateful to Keith Chater (John Innes Centre, Norwich) for his advice and for critically reading the manuscript.

References

Baysarowich, J., Koteva, K., Hughes, D.W., Ejim, L., Griffiths, E., Zhang, K., Junop, M., and Wright, G.D. 2008. Rifamycin antibiotic resistance by ADP-ribosylation: Structure and diversity of Arr. *Proc. Natl. Acad. Sci. USA* **105**, 4886–4891.

Bazan, J.F. and Koch-Nolte, F. 1997. Sequence and structural links between distant ADP-ribosyltransferase families, pp. 99–107. *In* Haag, F. and KochNolte, F. (eds.), ADP-ribosylation in animal tissues: Structure, function, and biology of mono (ADP-ribosyl) transferases and related enzymes. Plenum Press Div. Plenum Publishing Corp., New York, N.Y., USA.

Chater, K.F. 2006. *Streptomyces* inside-out: A new perspective on the bacteria that provide us with antibiotics. *Philos. Trans. R. Soc. Lond. B Biol. Sci.* **361**, 761–768.

Chater, K.F. and Losick, R. 1997. Mycelial life style of *Streptomyces coelicolor* A3(2) and its relatives, pp. 149–182. *In* Shapiro, J.A. and Dworkin, M. (eds.), Bacteria as multicellular organisms. Oxford University Press, London, UK.

Domenighini, M. and Rappuoli, R. 1996. Three conserved consensus sequences identify the NAD-binding site of ADP-ribosylating enzymes, expressed by eukaryotes, bacteria and T-even bacteriophages. *Mol. Microbiol.* **21**, 667–674.

Eastman, D. and Dworkin, M. 1994. Endogenous ADP-ribosylation during development of the prokaryote *Myxococcus xanthus*. *Microbiology-UK* **140**, 3167–3176.

Fernández-Moreno, M.A., Caballero, J.L., Hopwood, D.A., and Malpartida, F. 1991. The *act* cluster contains regulatory and antibiotic export genes, direct targets for translational control by the *bldA* tRNA gene of streptomyces. *Cell* **66**, 769–780.

Flärdh, K. and Buttner, M.J. 2009. *Streptomyces* morphogenetics: Dissecting differentiation in a filamentous bacterium. *Nat. Rev. Microbiol.* **7**, 36–49.

Geipel, U., Just, I., and Aktories, K. 1996. ADP-ribosylation of an approximately 70-kilodalton protein of *Klebsiella pneumoniae*. *Infect. Immun.* **64**, 1720–1723.

Gust, B., Challis, G.L., Fowler, K., Kieser, T., and Chater, K.F. 2003. PCR-targeted *Streptomyces* gene replacement identifies a protein domain needed for biosynthesis of the sesquiterpene soil odor geosmin. *Proc. Natl. Acad. Sci. USA* **100**, 1541–1546.

Han, S. and Tainer, J.A. 2002. The ARTT motif and a unified structural understanding of substrate recognition in ADP-ribosylating bacterial toxins and eukaryotic ADP-ribosyltransferases. *Int. J. Med. Microbiol.* **291**, 523–529.

Holbourn, K.P., Shone, C.C., and Acharya, K.R. 2006. A family of killer toxins - Exploring the mechanism of ADP-ribosylating toxins. *FEBS J.* **273**, 4579–4593.

Huh, J.W., Shima, J., and Ochi, K. 1996. ADP-ribosylation of proteins in *Bacillus subtilis* and its possible importance in sporulation. *J. Bacteriol.* **178**, 4935–4941.

Jouanneau, Y., Roby, C., Meyer, C.M., and Vignais, P.M. 1989. ADP-ribosylation of dinitrogenase reductase in *Rhodobacter capsulatus*. *Biochem.* **28**, 6524-6530.

Kieser, T.M., Bibb, J., Buttner, M.J., Chater, K.F., and Hopwood, D.A. 2000. Practical *Streptomyces* genetics, The John Innes Foundation, Norwich, UK.

Li, H., Jacques, P.E., Ghinet, M.G., Brzezinski, R., and Morosoli, R. 2005. Determining the functionality of putative Tat-dependent signal peptides in *Streptomyces coelicolor* A3(2) by using two different reporter proteins. *Microbiology-UK* **151**, 2189–2198.

Lowery, R.G. and Ludden, P.W. 1990. Endogenous ADP-ribosylation in prokaryotes, pp. 459–468. *In* Moss, J. and Vaughan, M. (eds.), ADP-ribosylating toxins and G-proteins. American Society for Microbiology, Washington, D.C., USA.

Ludden, P.W. 1994. Reversible ADP-ribosylation as a mechanism of enzyme regulation in prokaryotes. *Mol. Cell. Biochem.* **138**, 123–129.

Nagahama, M., Sakaguchi, Y., Kobayashi, K., Ochi, S., and Sakurai, J. 2000. Characterization of the enzymatic component of *Clostridium perfringens* iota-toxin. *J. Bacteriol.* **182**, 2096–2103.

Ochi, K., Penyige, A., and Barabás, G. 1992. The possible role of ADP-ribosylation in sporulation and streptomycin production by *Streptomyces griseus*. *J. Gen. Microbiol.* **138**, 1745–1750.

Penyige, A., Deák, E., Kálmánczhelyi, A., and Barabás, G. 1996. Evidence of a role for $NAD^{(+)}$-glycohydrolase and ADP-ribosyltransferase in growth and differentiation of *Streptomyces griseus* NRRL B-2682: Inhibition by m-aminophenylboronic acid. *Microbiology-UK* **142**, 1937–1944.

Penyige, A., Keserű, J., Fazakas, F., Schmelczer, I., Szirák, K., Barabás, G., and Biró, S. 2009. Analysis and identification of ADP-ribosylated proteins of *Streptomyces coelicolor* M145. *J. Microbiol.* **47**, 549–556.

Reinert, D.J., Carpusca, I., Aktories, K., and Schulz, G.E. 2006. Structure of the mosquitocidal toxin from *Bacillus sphaericus*. *J. Mol. Biol.* **357**, 1226–1236.

Ritter, H., Koch-Nolte, F., Marquez, V.E., and Schulz, G.E. 2003. Substrate binding and catalysis of ecto-ADP-ribosyltransferase

2.2 from rat. *Biochemistry* **42**, 10155–10162.

Sambrook, J., Fritsch, E.F., and Maniatis, T. 1989. Molecular cloning. A laboratory manual. Cold Spring Harbor Laboratory Press, Cold Spring Harbor, New York, N.Y., USA.

Serres, M.H. and Ensign, J.C. 1996. Endogenous ADP-ribosylation of proteins in *Mycobacterium smegmatis*. *J. Bacteriol.* **178**, 6074–6077.

Shima, J., Penyige, A., and Ochi, K. 1996. Changes in patterns of ADP-ribosylated proteins during differentiation of *Streptomyces coelicolor* A3(2) and its developmental mutants. *J. Bacteriol.* **178**, 3785–3790.

Stephenson, K. 2005. Sec-dependent protein translocation across biological membranes: Evolutionary conservation of an essential protein transport pathway. *Mol. Membr. Biol.* **22**, 17–28.

Sugawara, K., Dohmae, N., Kasai, K., Saido-Sakanaka, H., Okamoto, S., Takio, K., and Ochi, K. 2002. Isolation and identification of novel ADP-ribosylated proteins from *Streptomyces coelicolor* A3(2). *Biosci. Biotechnol. Biochem.* **66**, 2292–2296.

Ueda, K. and Hayaishi, O. 1985. ADP-ribosylation. *Annu. Rev. Biochem.* **54**, 73–100.

Vara, J., Lewandowska-Skarbek, M., Wang, Y.G., Donadio, S., and Hutchinson, C.R. 1989. Cloning of genes governing the deoxysugar portion of the erythromycin biosynthesis pathway in *Saccharopolyspora erythraea* (*Streptomyces erythreus*). *J. Bacteriol.* **171**, 5872–5881.

Watanabe, M., Enomoto, S., Takamura-Enya, T., Nakano, T., Koyama, K., Sugimura, T., and Wakabayashi, K. 2004. Enzymatic properties of pierisin-1 and its N-terminal domain, a guanine-specific ADP-ribosyltransferase from the cabbage butterfly. *J. Biochem.* **135**, 471–477.

Widdick, D.A., Dilks, K., Chandra, G., Bottrill, A., Naldrett, M., Pohlschroder, M., and Palmer, T. 2006. The twin-arginine translocation pathway is a major route of protein export in *Streptomyces coelicolor*. *Proc. Natl. Acad. Sci. USA* **103**, 17927–17932.

Zhang, R.G., Scott, D.L., Westbrook, M.L., Nance, S., Spangler, B.D., Shipley, G.G., and Westbrook, E.M. 1995. The three-dimensional crystal-structure of cholera-toxin. *J. Mol. Biol.* **251**, 563–573.